Research Square

Preprints are preliminary reports that have not undergone peer review.
They should not be considered conclusive, used to inform clinical practice,
or referenced by the media as validated information.

Ultrasound-mediated extracellular matrix-preserving detachment suppresses extrinsic aging of mesenchymal stromal cells

Chikahiro Imashiro

imashiro@pe.t.u-tokyo.ac.jp

The University of Tokyo

Fumiko Tomatsu

Canon Inc.

Jun Homma

Institute of Advanced Biomedical Engineering and Science, Tokyo Women's Medical University

https://orcid.org/0009-0001-1976-0670

Shunsuke Yamagata

The University of Tokyo

Hideharu Shimozawa

Canon Inc.

Shinsuke Mochizuki

Canon Inc.

Atsushi Nakamoto

Canon Inc.

Yoshikatsu Akiyama

Tokyo Women's Medical University (TWIns)

Tatsuya Shimizu

Tokyo Women's Medical University https://orcid.org/0000-0001-7601-4239

Article

Keywords:

Posted Date: July 20th, 2026

DOI: https://doi.org/10.21203/rs.3.rs-10390888/v1

License: This work is licensed under a Creative Commons Attribution 4.0 International License.
Read Full License

Additional Declarations: Yes there is potential Competing Interest. This work was supported by research funding from Canon Inc. F.T., H.S., S.M., and A.N. are employees of Canon Inc. C.I. and A.N. are inventors on patent applications related to the ultrasound-mediated, enzyme-free passaging technology. The remaining authors declare no competing interests.

Ultrasound-mediated extracellular matrix-preserving detachment suppresses extrinsic aging of mesenchymal stromal cells

Fumiko Tomatsu[†1], Jun Homma[†2], Shunsuke Yamagata[3], Hideharu Shimozawa[1], Shinsuke Mochizuki[1], Atsushi Nakamoto[1], Yoshikatsu Akiyama[2], Tatsuya Shimizu[2] & Chikahiro Imashiro*[3,2]

[†]These authors contributed equally to this work.

*Corresponding author

Chikahiro Imashiro

imashiro@pe.t.u-tokyo.ac.jp

1. Medical Business Operations, Canon Inc., 3-30-2 Shimomaruko, Ota-ku, Tokyo 146-8501, Japan.
2. Institute of Advanced Biomedical Engineering and Science, Tokyo Women's Medical University (TWIns), 8-1 Kawada-cho, Shinjuku-ku, Tokyo 162-8666, Japan.
3. Graduate School of Engineering, The University of Tokyo, 7-3-1 Hongo, Bunkyo-ku, Tokyo 113-8654, Japan.

Abstract

Large-scale expansion of mesenchymal stromal cells (MSCs) is essential for regenerative medicine. However, serial passaging is accompanied by progressive cellular aging and deterioration in cell quality. Conventional enzymatic passaging may accelerate this process by adding non-physiological stress beyond intrinsic replicative senescence. We developed an ultrasound-mediated, enzyme-free passaging system that enables complete and gentle detachment of MSCs while preserving the extracellular matrix and adhesion-associated structures. Ultrasound-mediated passaging maintained high cell viability and sustained proliferation over extended culture periods, resulting in higher cumulative cell yields than trypsin-based passaging. MSCs cultured under enzyme-free conditions preserved their spindle-shaped morphology, suppressed cell hypertrophy, and exhibited attenuated senescence-associated features, including reduced senescence-associated β-galactosidase activity and attenuated p53 induction. Ultrasound-mediated cell passaging did not compromise self-renewal capacity, differentiation potential, or the expression of stemness-associated markers compared with that induced by conventional trypsinization. Thus, passage-associated aging is predominantly due to procedure-induced extrinsic stress rather than intrinsic replicative limits.

Introduction

Mesenchymal stromal cells (MSCs) are widely used in regenerative medicine and cell-based therapies. However, their clinical application requires the production of a large number of cells, typically about 10^7–10^9 cells per treatment[1]. Achieving these high cell numbers necessitates long-term culture involving repeated passaging. Furthermore, MSCs progressively acquire senescence-associated phenotypes during serial passaging. This deterioration in cellular quality represents a major bottleneck for large-scale manufacturing and directly compromises therapeutic efficacy[2,3]. MSC senescence during long-term culture has been extensively documented. We hypothesized that this phenomenon arises from the interplay of two distinct components: intrinsic, physiological limitations associated with replicative history and extrinsic, non-physiological stresses imposed by the culture environment. However, the relative contributions of these components have not been experimentally separated. Therefore, the extent to which the intrinsic proliferative capacity of MSCs can be maintained under physiologically relevant conditions remains unclear.

Conventional trypsin-based passaging imposes multiple acute stresses on cells, including proteolytic disruption of cell–matrix interactions, loss of cell–substrate adhesion, and disruption of cytoskeletal organization[4]. These cytoskeletal perturbations regulate YAP activity, which is closely associated with p53 signaling and cellular senescence[5–7]. These procedure-induced perturbations are unlikely to occur *in vivo* and can act as extrinsic, non-physiological drivers of cellular aging. In contrast, intrinsic aging processes that accumulate with successive cell divisions, such as telomere shortening and replication-associated stress, are expected to impose fundamental limits on MSC proliferation. However, their quantitative contribution remains poorly defined[2,8,9]. Importantly, no experimental framework has been established to separate and independently evaluate intrinsic and extrinsic aging factors during MSC expansion. Consequently, the extent to which exogenous stress associated with conventional passaging has artificially constrained the apparent proliferative lifespan of MSCs remains unknown. This limitation largely stems from the absence of a passaging strategy that can reliably harvest cells without enzymatic treatment, thereby precluding the establishment of culture conditions that minimize non-physiological extrinsic stimuli.

We previously developed an enzyme-free cell detachment technique based on ultrasound, which enables cell harvesting from culture substrates without dissolving the extracellular matrix (ECM)[10–16]. Although the exact mechanism remains unclear, our findings indicate that the nonlinear effects of ultrasound facilitate cell detachment[17]. The enzyme-free approach preserves cytoskeletal organization and adhesion-related proteins during detachment and supports robust reattachment[18,19]. This ultrasound-mediated strategy suppresses procedure-induced, non-physiological extrinsic stress, thereby providing a unique experimental platform for maintaining MSC structural homeostasis and proliferative behavior in a more physiological state. This approach further enables a clearer assessment of the contribution of intrinsic aging processes.

In this study, we aimed to elucidate the mechanisms through which the suppression of passaging-induced stress affects senescence progression and the maintenance of stemness in MSCs using a newly designed ultrasound-mediated, enzyme-free passaging system that enables serial passaging under minimized extrinsic stress (Fig. 1), termed the Cellular Enzyme-free Passaging Ultrasound System (CEPUS). We further sought to evaluate the effectiveness and biological basis of ultrasound-mediated, enzyme-free passaging. Furthermore, we investigated the extent to which MSCs can intrinsically sustain their proliferative potential during long-term culture.

Results

Design and validation of CEPUS

We developed a cell detachment system, termed CEPUS, that combines ultrasound stimulation, mechanical tapping, and shaking (Fig. 2a). Each modality was designed to provide distinct physical cues: ultrasound induces high-frequency vibrations at the substrate surface, mechanical tapping excites global resonance modes of the culture dish, and shaking generates bulk fluid motion. The combination of these stimuli was designed based on conventional cell detachment procedures, in which mild mechanical perturbations such as pipetting and tapping are commonly applied. Combining these stimuli enhanced detachment efficiency in preliminary experiments.

The vibration characteristics of the culture substrate were evaluated using a laser Doppler vibrometer (LDV). The substrate exhibited a monotonic decrease in vibration velocity from the center toward the periphery, ranging from approximately 80 mm/s near the center to approximately 20 mm/s at the periphery (Fig. 2b). The velocity remained above the previously reported threshold for cell detachment across the measured region[13]. As shown in Fig. 2c, tapping generated relatively large substrate vibrations, with vibration velocities reaching approximately 30 mm/s. The time-domain vibration signal was subjected to fast Fourier transform (FFT) analysis to further characterize the frequency components of this tapping-induced motion. The resulting spectrum showed that the dominant frequency components were mainly distributed below approximately 6 kHz (Fig. 2d). In addition, shaking generated oscillatory motion of the culture dish with velocities reaching approximately 100 mm/s (Fig. 2e).

Ultrasound-mediated enzyme-free passaging enables complete and gentle cell detachment and promotes continuous MSC proliferation

Ultrasound stimulation induced complete and uniform detachment of MSCs. Before detachment, MSCs exhibited a typical spindle-shaped morphology (Fig. 3a), whereas no residual adherent cells were observed on the culture surface following ultrasound-mediated detachment (representative image

from passage 5; Fig. 3b). Quantitative evaluation of detachment efficiency demonstrated successful cell removal at all evaluated passages, indicating that ultrasound-mediated detachment was consistently achieved throughout serial passaging (Fig. 3c).

Immediately after ultrasound-mediated detachment, MSCs maintained high viability comparable to that observed in the trypsin-treated group (Fig. 3d). Since no enzymatic treatment was applied, the ECM component fibronectin was retained on the cell surface following detachment (Figs. 3e, f). These results indicate that ultrasound-mediated passaging enables gentle cell detachment without compromising cell viability or inducing ECM degradation.

The long-term proliferative capacity of MSCs was subsequently examined under serial passaging conditions. MSCs in the ultrasound (US) group continued to proliferate from the primary culture through passage 21, maintaining stable growth behavior throughout the culture period (N = 3 for passages up to P18; N = 2 for P19–P21) (Fig. 3g). The termination of culture at passages 18 and 21 was determined by the experimental design rather than by loss of proliferative potential, as cells remained proliferative until the final time points. In contrast, MSCs in the Trypsin group (N = 3) exhibited an earlier decline in proliferative capacity, with growth progressively plateauing during serial passaging. Comparison of cumulative cell yields revealed that the US group achieved substantially higher final cell numbers than the Trypsin group, exceeding a 10^8-fold difference in cumulative yield.

Collectively, these results demonstrate that ultrasound-assisted ultrasound-mediated enzyme-free passaging enables complete and minimally-invasive cell detachment while supporting the sustained proliferative capacity of MSCs during long-term culture.

Serial passage without enzymatic stress suppresses cellular senescence

Long-term serial passaging induced marked morphological changes in MSCs cultured using conventional trypsinization. Cells in the Trypsin group progressively exhibited increased size and a flattened morphology with advancing passages (Fig. 4a). In contrast, MSCs passaged using ultrasound-mediated enzyme-free passaging (US) retained a spindle-shaped morphology over extended culture periods and appeared morphologically consistent. Representative confocal images of actin filaments and nuclei were acquired for subsequent quantitative analysis of cytoskeletal and nuclear morphology (Fig. 4b).

To quantitatively assess these morphological changes, cell area, nuclear area, and nuclear aspect ratio were analyzed using two-way analysis of variance (ANOVA) with passaging method and passage

number as factors, followed by Tukey's post hoc test (Fig. 4c–e). Significant main effects of both passaging method and passage number were observed for cell area (Fig. 4c). In the Trypsin group, cell area increased significantly from passage 5 (P5) to passage 8 (P8), whereas no significant increase was detected in the US group. At P8, cells in the US group exhibited a significantly smaller cell area than those in the Trypsin group. Nuclear area analysis revealed a significant interaction between passaging method and passage number (Fig. 4d), with the US group showing a significantly smaller nuclear area than the Trypsin group at P8. Similarly, nuclear aspect ratio showed significant main effects of passaging method and passage number, as well as a significant interaction between these factors (Fig. 4e). The nuclear aspect ratio decreased from P5 to P8 in the Trypsin group, whereas no significant change was observed in the US group. Across all morphological parameters, significant differences were observed between the US and Trypsin groups at P8.

Senescence-associated β-galactosidase (SA-β-gal) staining further supported these observations. The number of SA-β-gal–positive cells increased substantially in the Trypsin group with serial passaging, whereas fewer positive cells were detected in the US group (Fig. 5a). Quantification of SA-β-gal–positive cells confirmed a passage-dependent increase in senescence in the Trypsin group, whereas this increase was attenuated in the US group (Fig. 5b).

Consistent with these findings, western blot analysis revealed a passage-dependent increase in a p53-immunoreactive band in the Trypsin group, whereas this band remained comparatively stable in the US group (Fig. 5c). Antibody specificity analyses indicated that this band most likely represents a p53 family species, potentially Δ40p53 (a p53 isoform reported to engage senescence-associated signaling). Detailed characterization is provided in Supplementary Note 1.

Collectively, these morphological and molecular indicators demonstrate a consistent trend in which senescence-associated changes accumulate during serial passaging with trypsinization, whereas ultrasound-mediated enzyme-free passaging suppresses the progression of these changes.

Stemness is maintained after serial enzyme-free passaging

To assess the self-renewal capacity of MSCs after serial passaging, colony formation assays were performed at P8. Qualitatively, MSCs passaged using ultrasound-mediated enzyme-free detachment (US) formed more colonies than those passaged using trypsinization (Trypsin) (Fig. 6a; see Supplementary Fig. 2 for complete plate images from all independent experiments). Colony area did not differ significantly between the two groups (Fig. 6b), whereas the number of colonies was

significantly higher in the US group (Fig. 6c). These results indicate that ultrasound-mediated enzyme-free passaging preserves the clonogenic growth potential of MSCs after serial passaging, supporting the maintenance of stemness at this passage.

The maintenance of multipotency was assessed by tri-lineage differentiation assays using MSCs at P8. MSCs in the US group exhibited mineralized matrix deposition (Fig. 6d), lipid droplet formation (Fig. 6e), and glycosaminoglycan production (Fig. 6f), demonstrating characteristic differentiation toward the osteogenic, adipogenic, and chondrogenic lineages, respectively.

Expression of stemness-associated surface markers was further examined by western blot analysis. At P4, no apparent differences in the expression levels of CD90 or CD73 were observed between the US and Trypsin groups (Fig. 6g, h). In contrast, at P8, CD90 expression remained comparable between the two groups (Fig. 6i), whereas CD73 expression showed a tendency toward lower levels in the Trypsin group than in the US group, although the difference did not reach statistical significance (Fig. 6j).

Collectively, these results indicate that ultrasound-mediated enzyme-free passaging maintains the clonogenic growth capacity and tri-lineage differentiation potential of MSCs at P8.

Discussion

In this study, we developed an ultrasound-mediated enzyme-free passaging system. We further comprehensively evaluated how conventional trypsin-based passaging and the proposed enzyme-free approach affect the long-term culture of MSCs. Ultrasound-mediated passaging enabled high cell recovery and viability, preserved spindle-shaped cell morphology during extended serial passaging, and suppressed cell hypertrophy. Senescence-associated signals, including increased SA-β-gal activity and p53-associated signaling, are widely used markers of cellular senescence in MSCs[20,21]. These signals were attenuated in this study, whereas markers related to stemness were maintained. Multiple independent indicators, including cellular morphology, cytoskeletal organization, senescence-associated signaling, and stem cell-associated functional properties, exhibited consistently favorable changes. This suggests that enzyme-free passaging can support the maintenance of MSC structural homeostasis and functional quality over prolonged culture periods. Furthermore, MSCs expanded using CEPUS achieved cell numbers far exceeding those typically required for clinical administration (10^7–10^9 cells)[1,22], reaching a final yield of 6×10^{13} cells. This finding suggests that minimizing procedure-induced extrinsic stress may allow the intrinsic proliferative potential of MSCs to become more apparent. However, this does not imply that replicative senescence is avoided. Thus, the progression of intrinsic aging processes must be considered separately.

The suppression of senescence-associated signals observed with ultrasound-mediated passaging is likely attributable to the reduction of procedure-induced extrinsic stress arising from the disruption of adhesion structures and the loss of cytoskeletal tension during passaging. Trypsin treatment leads to degradation of the ECM and loss of cell adhesion, causing cells to experience a contracted, non-adherent state for a certain period after detachment[23–25]. In contrast, ultrasound-mediated detachment shortens the time required for cell reattachment compared with enzymatic detachment[10,18]. This has been attributed to the preservation of the ECM and adhesion-related structures during detachment. As a result, the duration over which cells experience mechanical conditions distinct from those of adherent cells is likely reduced. Consistent with observations in cell sheet engineering, prolonged loss of adhesion induces cellular contraction[19]. Therefore, differences in such procedure-induced stress profiles may affect cytoskeletal and nuclear morphology, as well as the progression of senescence-associated signaling. Consistently, ultrasound-mediated passaging suppressed increases in SA-β-gal activity and p53-associated signaling, whereas self-renewal capacity was preserved. Moreover, tri-lineage differentiation assays, widely accepted as a defining functional criterion of MSCs, confirmed that differentiation potential was not lost following ultrasound-mediated passaging[26]. Importantly, these findings indicate that the suppression of senescence-associated signals under ultrasound-mediated passaging did not arise from the expansion of aberrant or functionally compromised cells. Rather, it occurred while preserving the defining characteristics of MSCs. Together, these findings support the interpretation that procedure-induced extrinsic stress is a major contributor to senescence-associated changes observed during conventional passaging. This study focused on p53 as a downstream indicator of senescence-associated signaling. However, the involvement of upstream mechanotransduction pathways, including YAP/TAZ, in mediating the effects of procedure-induced cytoskeletal disruption remains to be examined in future studies.

These findings further suggest that the phenomenon traditionally described as “passage-dependent aging” of MSCs is not a single, uniform biological process. Instead, it may comprise at least two distinct components. Cell area increased significantly under trypsin-based passaging, and nuclear aspect ratio decreased with advancing passages. The nuclear area at later passages (P8) was significantly larger than that observed under ultrasound-mediated passaging. These morphological changes likely reflect the cumulative effects of repeated exposure to procedure-induced extrinsic stress, including adhesion loss and cytoskeletal reorganization, which promote the manifestation of senescence-associated phenotypes[5–7]. These cytoskeletal perturbations are expected to affect nuclear morphology, as cytoskeletal tension regulates nuclear shape through contractile perinuclear actin structures coupled to the nucleus[27]. Reductions in nuclear aspect ratio have also been reported in senescent MSCs driven by intrinsic aging mechanisms, such as metabolic dysregulation[28]. This suggests that similar nuclear morphological changes can arise from both extrinsic and intrinsic aging

processes. In contrast, no significant passage-dependent changes in cell area or nuclear aspect ratio were observed under ultrasound-mediated passaging. Additionally, the nuclear area remained smaller than that of the Trypsin group at later passages. These findings indicate that many morphological changes collectively referred to as “passaging-induced aging” are not necessarily inevitable when extrinsic stress is relatively minimized. Nevertheless, even under ultrasound-mediated passaging, changes associated with increasing numbers of cell divisions were not eliminated, suggesting the presence of intrinsic aging components inherent to MSCs that progress in a division-dependent manner. This study provides an experimental framework for the separate evaluation of extrinsic, procedure-induced aging and intrinsic, replication-associated aging during long-term MSC culture. Thus, it offers a new conceptual perspective on MSC aging that was previously considered a single biological process.

Although this study focused on MSCs, the underlying principle of ultrasound-mediated enzyme-free passaging is not inherently cell-type-specific. In our previous studies, we demonstrated that ultrasound-mediated detachment preserves adhesion-related structures and supports efficient reattachment and proliferation[10,16,18]. In this sense, the current findings highlight an operational strategy rather than a phenomenon restricted to MSC biology. In addition, because ultrasound stimulation is a purely physical and externally controllable modality, it is inherently compatible with a wide range of materials-based culture systems, including temperature-responsive polymers and metallic substrates[29,30]. This compatibility is particularly advantageous in the context of automated cell culture and manufacturing, where closed systems, process stability, and reproducible cell handling are essential requirements. Together, these characteristics suggest that ultrasound-mediated enzyme-free passaging may serve as a flexible and transferable component in the design of future cell culture and manufacturing processes, particularly in contexts where the preservation of cellular structural integrity is required during expansion. Nevertheless, this study has several limitations. Although ultrasound-mediated enzyme-free passaging is expected to be broadly applicable, the experimental validation was limited to MSCs and a specific culture system. Future studies should further clarify the mechanisms underlying ultrasound-mediated cell detachment and the suppression of passaging-associated aging, and evaluate the applicability of this approach across different cell types, culture substrates, and experimental conditions.

In summary, we developed an ultrasound-mediated enzyme-free passaging system and used it to evaluate the effects of procedure-induced extrinsic stress during long-term MSC expansion in comparison with conventional trypsin-based passaging. Ultrasound-mediated passaging enabled cell harvesting while preserving the extracellular matrix and adhesion-associated structures, maintained high cell viability and proliferative capacity, and suppressed increases in cell hypertrophy, SA-β-gal activity, and p53-associated signaling. In addition, self-renewal capacity, tri-lineage differentiation

potential, and stemness-associated markers were not substantially impaired. These findings indicate that at least part of the senescence-associated changes observed during serial MSC passaging is not solely attributable to inevitable intrinsic aging associated with cell division but also to extrinsic stress caused by enzymatic treatment and disruption of adhesion structures. This study provides an experimental framework for distinguishing intrinsic and extrinsic components of MSC aging and suggests a potential cell manufacturing strategy for large-scale expansion while preserving cellular structural integrity.

Methods

Ultrasound stimulation setup for CEPUS

Ultrasound stimulation was generated using a Langevin-type transducer (HEC-422002; Honda Electronics, Japan), which was mounted inside CEPUS. Vibrations were transmitted to the culture dish through a custom-designed elastic coupling material[31]. The cross-sectional view is shown in Supplementary Fig. 3.

Validation of CEPUS

Vibrations induced by ultrasound stimulation, mechanical tapping, and shaking were characterized using LDV to quantitatively validate the physical stimuli generated by CEPUS. Reflective tape (Scotchlite; 3M, USA) was applied to all measurement points to enhance signal detection.

The vibration characteristics of the culture substrate under ultrasound stimulation were measured using an LDV (LV-1800; Ono Sokki, Japan). Vibration velocity was measured at multiple positions along a radial line extending from the center of the culture dish toward the periphery (0–15 mm). Measurements were repeated five times (N = 5) at each position, and the mean and standard deviation are presented.

The vibration induced by mechanical tapping was measured at the center of the culture dish using an LDV (LV-1800; Ono Sokki, Japan) (N = 10). FFT was applied to each acquired vibration signal individually, and the resulting spectra were averaged to analyze the frequency components. The raw data are provided in Supplementary Fig. 4.

For shaking, vibration measurements were performed at the side surface of CEPUS using an LDV system (LV-50Z; Pro-Net Co., Ltd., Japan), as the motion of the device was directly transmitted to the culture vessel.

Ethics

All animal experiments were approved by the Ethics Committee for Animal Experimentation of Tokyo Women's Medical University (Approval No. AE24-109), were performed according to the Guidelines

of Tokyo Women's Medical University on Animal Use, and were conducted in compliance with the ARRIVE guidelines for the care and use of laboratory animals.

All animals were housed in individual cages and maintained under controlled temperature and humidity conditions (20–24 °C and 40–60% relative humidity) with a 12-h light/dark cycle. Animals were provided with free access to food and water. Animals were euthanized by exsanguination under 5% isoflurane in accordance with the American Veterinary Medical Association euthanasia guidelines.

Isolation of mesenchymal stromal cells

MSCs were isolated from the inguinal adipose tissue of male Sprague–Dawley rats (Jcl:SD; 280–400 g; CLEA Japan) as previously described[32]. Briefly, excised adipose tissue was digested with 0.05% collagenase type II (Worthington Biochemical Corporation, USA) for 40 min at 37 °C using an automated tissue dissociation system (gentleMACS Octo Dissociator; Miltenyi Biotec, Bergisch Gladbach, Germany). The resulting cell suspension was passed through a 40-μm cell strainer and centrifuged at 800 × *g* for 5 min at room temperature (20–24 °C). The cell pellet was resuspended and plated onto 100-mm culture dishes, and the cells were cultured at 37 °C in a humidified atmosphere containing 5% CO_2 in complete medium consisting of DMEM/F12 supplemented with GlutaMAX™ (Thermo Fisher Scientific, USA), 10% fetal bovine serum (Japan Bio Serum Co., Ltd., Japan), and 1% penicillin–streptomycin (FUJIFILM Wako, Japan). After 24 h, the medium was replaced to remove non-adherent cells. Cells were passaged between days 6 and 10 and transferred to new culture dishes. MSCs were cryopreserved at −150 °C at passage 2. The cryopreserved MSCs were subsequently thawed and seeded onto culture dishes.

Cell culture

Rat MSCs were seeded onto 35-mm culture dishes (Greiner Bio-One GmbH, Germany) at a density of either 5.0×10^4 or 2.5×10^4 cells per dish. Cells were cultured in complete medium consisting of DMEM/F12 (Gibco, Thermo Fisher Scientific) supplemented with 10% fetal bovine serum (Nichirei Biosciences Inc., Japan) and 1% penicillin–streptomycin. Cells were maintained at 37 °C in a humidified atmosphere containing 5% CO_2 for 3–4 days before passaging. In all experiments, MSCs were expanded using trypsin-based passaging up to passage 3 (P3); from P3 onward, cells were divided into two groups and passaged either by conventional trypsinization or ultrasound-mediated, enzyme-free detachment. After the culture period, cells were detached either using 0.5% (w/v) trypsin–5.3 mmol/L EDTA·4Na solution without phenol red (FUJIFILM Wako) or by ultrasound-mediated, enzyme-free detachment.

Enzyme-free passaging procedure

After 3–4 days of culture, cells were washed three times with 1× phosphate-buffered saline (PBS;

Gibco). Subsequently, 2 mL of PBS was added to each dish, and the cells were incubated at 37 °C for 5 min.

Cell detachment was then performed using CEPUS for 3 min under the following conditions. Ultrasound stimulation was applied at an input voltage of 45 V with a downward frequency-sweep mode, a sweep range of 37–36 kHz, and a sweep duration of 1 s. In addition, mechanical tapping was applied at a frequency of 5 Hz using a spring with a spring constant of 0.05 N/mm and an initial compression of 0 mm. Horizontal shaking of the culture dish was applied simultaneously at a frequency of 1.3 Hz.

Cell viability and proliferation assay

Cell viability and total cell number were evaluated after cell detachment by either trypsin treatment or ultrasound-mediated, enzyme-free passaging. Detached cells were stained with trypan blue (Invitrogen) and counted using a hemocytometer to determine total and viable cell numbers. Cell viability was calculated as the percentage of trypan blue–negative cells relative to the total cell count.

Fluorescence staining

The proportion of SA-β-Gal–positive cells was evaluated using SPiDER-β-Gal (DOJINDO LABORATORIES, Japan). Cultured cells were washed with 2 mL of Hank's Balanced Salt Solution (HBSS; Gibco), followed by the addition of 0.75 mL of bafilomycin A1 working solution and incubation at 37 °C for 1 h. Subsequently, 0.75 mL of SPiDER-β-Gal working solution was added, and the cells were incubated at 37 °C for 35 min. After washing with PBS, the cells were detached using trypsin, collected, and centrifuged at 200 × *g* for 3 min. The resulting cell pellet was resuspended in HBSS. The cell suspension was loaded onto Countess Cell Counting Chamber Slides (Invitrogen, Thermo Fisher Scientific). Imaging was performed on a fluorescence microscope (ECLIPSE Ti2; Nikon, Japan) using DAPI and FITC filter sets with an exposure time of 200 ms and an analog gain of ×2.2.

Cells detached at P4 were seeded onto 12-well plates (Greiner Bio-One GmbH) at a density of 5.6×10^4 cells per well, cultured for 3 days at 37 °C in a humidified atmosphere containing 5% CO_2, and analyzed at P5. Cells from P7 were similarly treated and analyzed at P8. After washing with PBS, the cells were fixed with 4% paraformaldehyde for 15 min and permeabilized with 0.1% Triton X-100 for 15 min at room temperature (24–26 ℃).

The cells were then stained with rhodamine–phalloidin (R415; Invitrogen) and Hoechst 33342 (H342; DOJINDO LABORATORIES) for 30 min at room temperature (24–26 ℃). After washing twice with PBS, fluorescence images were acquired using a fluorescence microscope (ECLIPSE Ti2; Nikon).

Fluorescence images were analyzed using ImageJ (version 1.54p; NIH). For each biological replicate, multiple randomly selected fields were analyzed under identical imaging and analysis conditions. Cell area, nuclear area, and nuclear aspect ratio were quantified at the single-cell level and first averaged within each biological replicate. The resulting replicate means were then used for statistical analyses.

Western blot analysis

For p53 analysis, proteins were extracted directly from adherent cultured cells before cell detachment using CelLytic™ M reagent (Sigma-Aldrich, USA) according to the manufacturer's instructions. For analyses of fibronectin and surface markers (CD73 and CD90), proteins were extracted from cells after detachment. After denaturation with sodium dodecyl sulfate (SDS), equal amounts of protein were separated by SDS–polyacrylamide gel electrophoresis using 4–20% Tris–glycine gels (Invitrogen) and transferred onto polyvinylidene difluoride membranes (Invitrogen).

Membranes were blocked with Blocking One (Nacalai Tesque, Japan) for 30 min at room temperature (24–26 °C) and subsequently incubated with primary antibodies for 3 h at room temperature (24–26 °C). The following primary antibodies were used: anti-p53 (rabbit polyclonal, 10442-1-AP, 1:1000; Proteintech, USA), anti-fibronectin (mouse monoclonal, sc-271098, 1:500; Santa Cruz Biotechnology, USA), anti-CD73 (rabbit monoclonal, #13160, 1:300; Cell Signaling Technology), anti-CD90 (mouse monoclonal, sc-19614, 1:100; Santa Cruz Biotechnology), and anti-GAPDH (rabbit polyclonal, 10494-1-Ig, 1:1000; Proteintech).

After washing, membranes were incubated with Alexa Fluor™ Plus 647-conjugated anti-mouse IgG (goat polyclonal, A32728, 1:10000; Invitrogen) and Alexa Fluor™ Plus 555-conjugated anti-rabbit IgG (goat polyclonal, A32732, 1:10000; Invitrogen) for 1 h at room temperature (24–26 °C). Protein bands were detected using the iBright Imaging System (Invitrogen), and band intensities were quantified using iBright Analysis Software (Invitrogen). GAPDH was used as the loading control.

Uncropped full-length images of all western blot membranes are provided in Supplementary Figs. 1 and 5.

Colony assay

Cells at passage 7 (P7) were detached by either trypsin treatment or ultrasound-mediated, enzyme-free passaging and evaluated at passage 8 (P8). A total of 1.0×10^3 cells were seeded onto 100-mm tissue culture dishes (Greiner Bio-One GmbH). Cells were cultured at 37 °C in a humidified atmosphere containing 5% CO_2, with the medium changed every 3–4 days. After 10 days of culture, the dishes were washed with PBS and fixed with 4% paraformaldehyde. The dishes were then washed with PBS and stained with crystal violet staining solution (Kanto Chemical Co., Inc., Japan) for 10 min at room temperature (24–26 °C). After washing with PBS, colonies with a diameter >2 mm were counted.

Colony diameters were individually verified using Microsoft PowerPoint before counting. Colony areas were quantified using ImageJ. For area analysis, colonies that were visibly fused or overlapped with adjacent colonies were excluded from measurement to avoid overestimation of individual colony size. However, for colony number quantification, fused colonies were counted as individual colonies when distinct colony origins were visually identifiable.

Tri-lineage differentiation assays

Cells at P7 were subjected to adipogenic, osteogenic, or chondrogenic differentiation assays at P8.

For adipogenic differentiation, cells were detached by ultrasound-mediated, enzyme-free passaging and seeded onto 12-well plates (Greiner Bio-One GmbH) at a density of 4.0×10^4 cells per well. Cells were cultured at 37 °C in a humidified atmosphere containing 5% CO_2, with the medium changed every 3–4 days. Upon reaching confluence, the culture medium was replaced with complete adipogenic differentiation medium (A1007001; StemPro Adipogenesis Differentiation Basal Medium supplemented with StemPro Adipogenesis Supplement; Thermo Fisher Scientific), and cells were cultured for 3 weeks, with the medium changed every 3–4 days. After differentiation, cells were washed with PBS, stained with Oil Red O, washed with PBS, and observed under a light microscope.

For osteogenic differentiation, P7 cells were detached by ultrasound-mediated, enzyme-free passaging and seeded onto 0.1% gelatin-coated 12-well plates (Greiner Bio-One GmbH) at a density of 2.0×10^4 cells per well. Cells were cultured at 37 °C in a humidified atmosphere containing 5% CO_2, with the medium changed every 3–4 days. When the cultures reached approximately 90% confluence, the medium was replaced with osteogenic differentiation medium (A1007201; StemPro Osteocyte/Chondrocyte Differentiation Basal Medium supplemented with StemPro Osteogenesis Supplement; Thermo Fisher Scientific), and the cells were cultured for 3 weeks, with the medium changed every 3–4 days. After differentiation, cells were washed with PBS, stained with Alizarin Red (ARD-A1; PG Research, Japan), washed with PBS, and observed under a light microscope.

For chondrogenic differentiation, P7 cells detached by ultrasound-mediated enzyme-free passaging were transferred into 15-mL centrifuge tubes at 1.8×10^5 cells per tube. After washing, the cells were centrifuged at 200 × *g* for 3 min at room temperature (24–26 ℃) to form pellets and incubated in chondrogenic differentiation medium (A1007101; StemPro Osteocyte/Chondrocyte Differentiation Basal Medium supplemented with StemPro Chondrogenesis Supplement; Thermo Fisher Scientific) at 37 °C in a humidified atmosphere containing 5% CO_2 for 24 h. The pellets were then cultured for 3 weeks, during which the medium was changed every 3–4 days. After culture, the pellets were washed with PBS, fixed with 4% paraformaldehyde, stained with Alcian Blue staining solution (pH 2.5; 37154-15; Nacalai Tesque), washed with PBS, and observed under a light microscope.

Statistical analysis

Cell area, nuclear area, and nuclear aspect ratio (Fig. 4) were analyzed using two-way ANOVA with passage number (P5 and P8) and passaging method (trypsin and ultrasound) as fixed factors, followed by Tukey's post hoc test. For pairwise comparisons between two independent groups, including the analyses shown in Fig. 3e, f, and Fig. 6b, c, and g–j, unpaired, two-tailed t-tests with Welch's correction were used. For all quantitative analyses, statistical tests were performed using the mean values of independent biological replicates rather than individual cells. Detailed statistical results are provided in Supplementary Tables 1–4. The significance threshold was set at $P < 0.05$. All analyses were performed using GraphPad Prism (version 10; GraphPad Software, USA).

Acknowledgements

The Japan Science and Technology Agency (JST) FOREST Program (Grant No. JPMJFR244G) supported this work.

Author contributions

F.T., J.H., and C.I. conceived the study. F.T., J.H., C.I., Y.A., and T.S. designed the study. F.T. performed the long-term serial passaging experiments, cell viability and proliferation assays, and western blot analyses. F.T. and J.H. performed MSC culture, senescence assays, differentiation assays, and other related biological experiments. S.Y. performed the physical characterization and validation of the ultrasound-mediated enzyme-free passaging system. H.S., S.M., and A.N. designed, developed, and technically validated CEPUS. F.T., J.H., S.Y., C.I., and Y.A. analyzed the data. Y.A. and T.S. contributed to the interpretation of MSC biology and the implications of the findings for cell manufacturing and regenerative medicine. T.S. provided experimental facilities and research resources. C.I., T.S., Y.A., and J.H. acquired funding. C.I. and T.S. supervised the project. F.T., J.H., and C.I. wrote the original draft. T.S. and C.I. reviewed and edited the manuscript. All authors discussed the results and approved the final manuscript.

Competing interests

This work was supported by research funding from Canon Inc. F.T., H.S., S.M., and A.N. are employees of Canon Inc. C.I. and A.N. are inventors on patent applications related to the ultrasound-mediated, enzyme-free passaging technology. The remaining authors declare no competing interests.

Materials & Correspondence

Correspondence and requests for materials should be addressed to Chikahiro Imashiro.

Data availability

The data supporting the findings of this study are available within the article and its Supplementary Information. Source data are provided with this paper. Additional raw data are available from the corresponding author upon reasonable request.

References

Pittenger, M. F. et al. Mesenchymal stem cell perspective: Cell biology to clinical progress. *NPJ Regen. Med.* **4**, 22 (2019).

Wagner, W. et al. Replicative senescence of mesenchymal stem cells: A continuous and organized process. *PLoS One.* **3**, e2213 (2008).

Weng, Z. et al. Mesenchymal stem/stromal cell senescence: Hallmarks, mechanisms, and combating strategies. *Stem Cells Transl. Med.* **11**, 356–371 (2022)

Reddig, P. J. & Juliano, R. L. Clinging to life: Cell to matrix adhesion and cell survival. *Cancer Metastasis Rev.* **24**, 425–439 (2005).

Aragona, M. et al. A mechanical checkpoint controls multicellular growth through YAP/TAZ regulation by actin-processing factors. *Cell.* **154**, 1047–1059 (2013).

Dupont, S. et al. Role of YAP/TAZ in mechanotransduction. *Nature* **474**, 179–183 (2011).

Xie, Q. et al. YAP/TEAD-mediated transcription controls cellular senescence. *Cancer Res.* **73**, 3615–3624 (2013).

Parsch, D., Fellenberg, J., Brümmendorf, T. H., Eschlbeck, A. M. & Richter, W. Telomere length and telomerase activity during expansion and differentiation of human mesenchymal stem cells and chondrocytes. *J. Mol. Med. (Berl)* **82**, 49–55 (2004).

López-Otín, C., Blasco, M. A., Partridge, L., Serrano, M. & Kroemer, G. The hallmarks of aging. *Cell* **153**, 1194–1217 (2013).

van Delft, J. et al. Spheroid cell aggregation enhanced by enzyme-free ultrasound-detached cells. *Adv. Biol.* (*Weinh)* **9**, e00092 (2025).

Imashiro, C. et al. Detachment of cell sheets from clinically ubiquitous cell culture vessels by ultrasonic vibration. *Sci. Rep.* **10**, 9468 (2020).

Tauchi, H. et al. Effective and intact cell detachment from a clinically ubiquitous culture flask by combining ultrasonic wave exposure and diluted trypsin. *Biotechnol. Bioprocess Eng.* **24**, 536–543 (2019).

Kurashina, Y. et al. Enzyme-free cell detachment mediated by resonance vibration with temperature modulation. *Biotechnol. Bioeng.* **114**, 2279–2288 (2017).

Inui, T., Kurashina, Y., Imashiro, C. & Takemura, K. Method of localized removal of cells using a bolt‐clamped Langevin transducer with an ultrasonic horn. *Eng. Life Sci.* **19**, 575–583 (2019).

Inui, T. et al. Focused surface acoustic wave locally removes cells from culture surface. *Lab Chip* **21**, 1299–1306 (2021).

Kuriyama, T. et al. Detachment of RAW264.7 macrophages from a culture dish using ultrasound excited by a Langevin transducer. *J. Biosci. Bioeng.* **131**, 320–325 (2021).

Imashiro, C., Mei, J., Friend, J. & Takemura, K. Quantifying cell adhesion through forces generated by acoustic streaming. *Ultrason. Sonochem.* **90**, 106204 (2022).

Kurashina, Y. et al. Enzyme-free release of adhered cells from standard culture dishes using intermittent ultrasonic traveling waves. *Commun. Biol.* **2**, 393 (2019).

Imashiro, C. & Shimizu, T. Fundamental technologies and recent advances of cell-sheet-based tissue engineering. *Int. J. Mol. Sci.* **22**, 425 (2021).

Campisi, J. & D'Adda Di Fagagna, F. Cellular senescence: When bad things happen to good cells. *Nat. Rev. Mol. Cell Biol.* **8**, 729–740 (2007).

Dimri, G. P. et al. A biomarker that identifies senescent human cells in culture and in aging skin in vivo. *Proc. Natl Acad. Sci. U. S. A.* **92**, 9363–9367 (1995).

Galipeau, J. & Sensébé, L. Mesenchymal stromal cells: Clinical challenges and therapeutic opportunities. *Cell Stem Cell* **22**, 824–833 (2018).

Chen, C. S., Mrksich, M., Huang, S., Whitesides, G. M. & Ingber, D. E. Geometric control of cell life and death. *Science* **276**, 1425–1428 (1997).

Hynes, R. O. Cell adhesion: Old and new questions. *Trends Cell Biol.* **9**, M33–M37 (1999).

Lordon, B., Campion, T., Gibot, L. & Gallot, G. Impact of trypsin on cell cytoplasm during detachment of cells studied by terahertz sensing. *Biophys. J.* **123**, 2476–2483 (2024).

Dominici, M. et al. Minimal criteria for defining multipotent mesenchymal stromal cells. The International Society for Cellular Therapy position statement. *Cytotherapy* **8**, 315–317 (2006).

Khatau, S. B. et al. A perinuclear actin cap regulates nuclear shape. *Proc. Natl Acad. Sci. U. S. A.* **106**, 19017–19022 (2009).

Sun, Y. et al. MiR-34a-HK1 signal axis retards bone marrow mesenchymal stem cell senescence via ameliorating glycolytic metabolism. *Stem Cell Res. Ther.* **15**, 238, (2024).

Imashiro, C. et al. Titanium culture vessel presenting temperature gradation for the thermotolerance estimation of cells. *Cyborg Bionic Syst.* **4**, 0049 (2023).

Matsuzaki, J., Akiyama, Y., Imashiro, C., Shimizu, T. & Komotori, J. et al. Reusable temperature-responsive cell-culture surfaces using poly(N-isopropylacrylamide)-grafted Ti–6Al–4V alloy. *Results Chem.* **28**, 103529 (2026).

Miura, J. & Yamamoto, Y., Tsubaki, K., Nakamoto, A., Sekiguchi, Y. JP Patent Application 2026-004196, (2026).

Homma, J., Sekine, H., Matsuura, K., Kobayashi, E. & Shimizu, T. Mesenchymal stem cell sheets exert antistenotic effects in a rat arterial injury model. *Tissue Eng. Part A* **24**, 1545–1553 (2018).

Figure

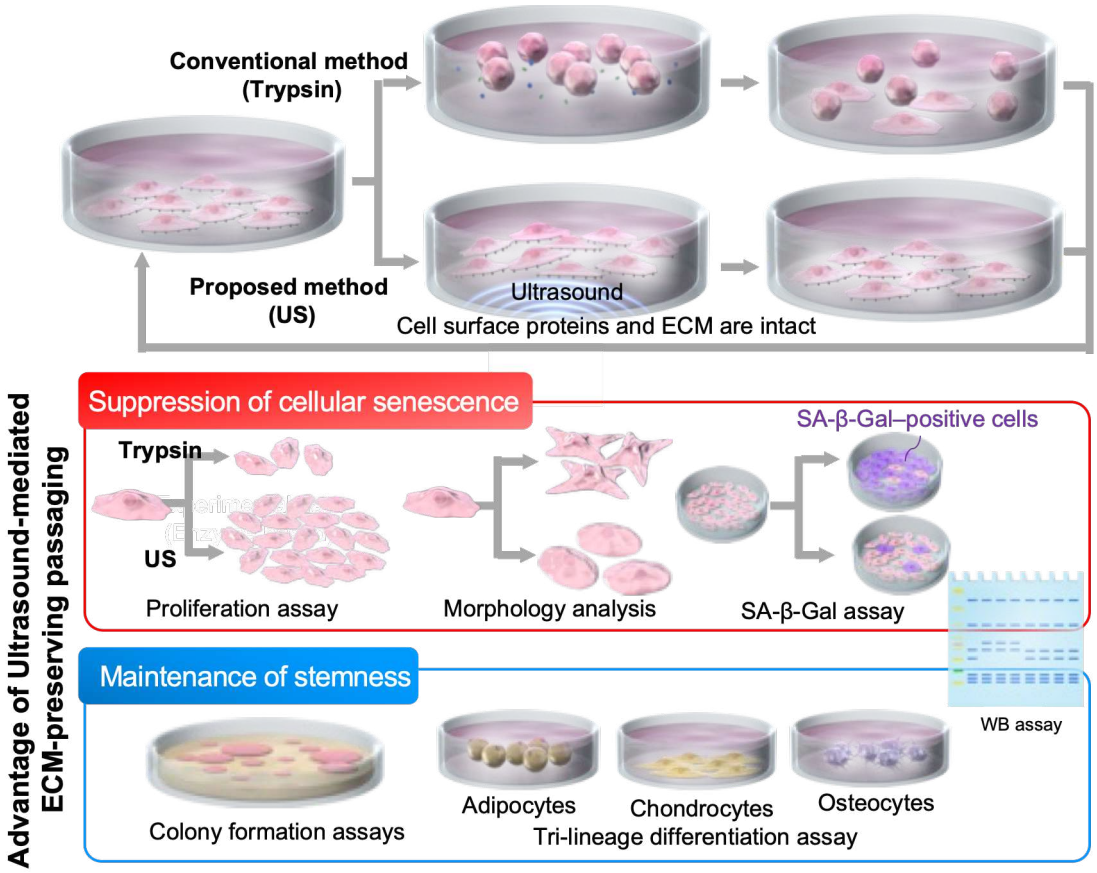
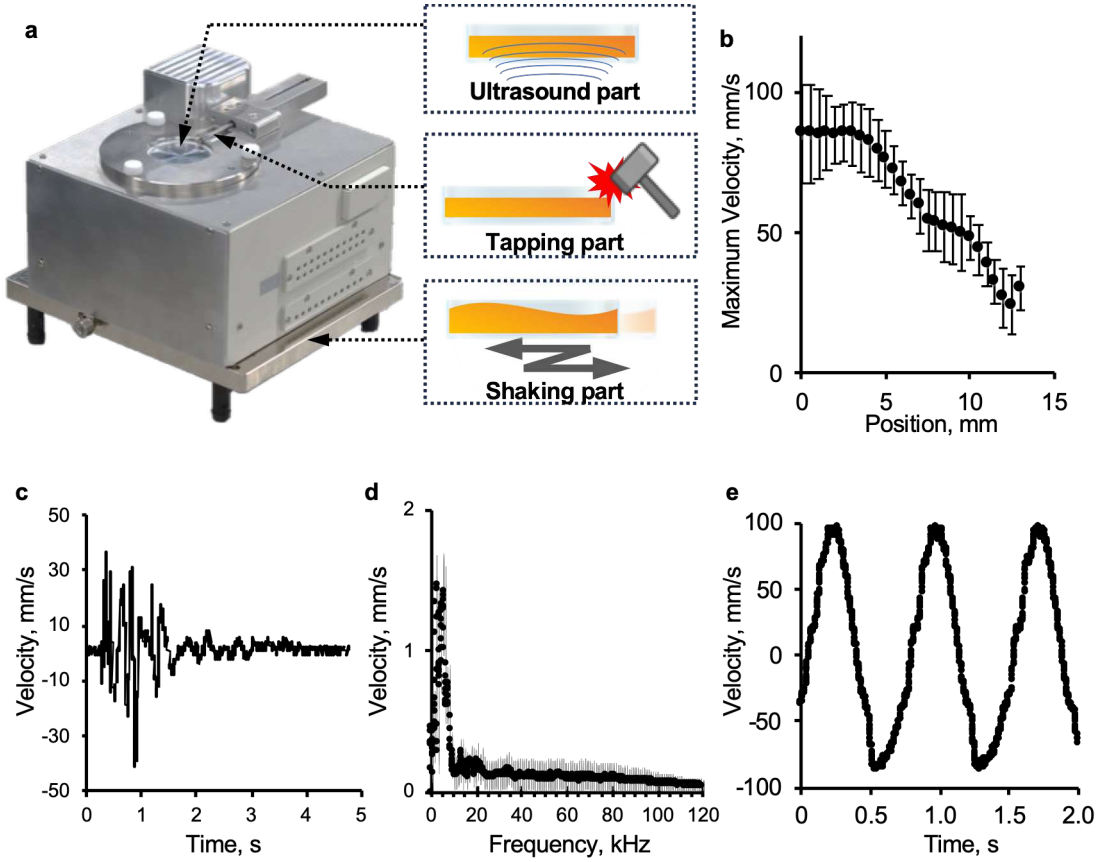


Fig. 1 | Overview of the ultrasound-mediated enzyme-free passaging strategy and experimental design.

Schematic illustration of the ultrasound-mediated enzyme-free passaging strategy and the experimental readouts examined in this study.



585

586 **Fig. 2 | Design and mechanical characterization of the developed device.**

587 (a) Photograph of the developed device and schematic illustration of the mechanical stimuli applied
588 to the culture dish. (b) Vibration velocity of the substrate induced by ultrasound stimulation (N = 5).
589 (c) Representative time-domain vibration signal of the culture dish induced by mechanical tapping.
590 (d) Frequency spectrum of tapping-induced vibrations obtained by fast Fourier transform (FFT) of
591 individually measured signals followed by averaging (N = 10). (e) Velocity of the shaking motion
592 measured at the device side surface (N = 1).

593

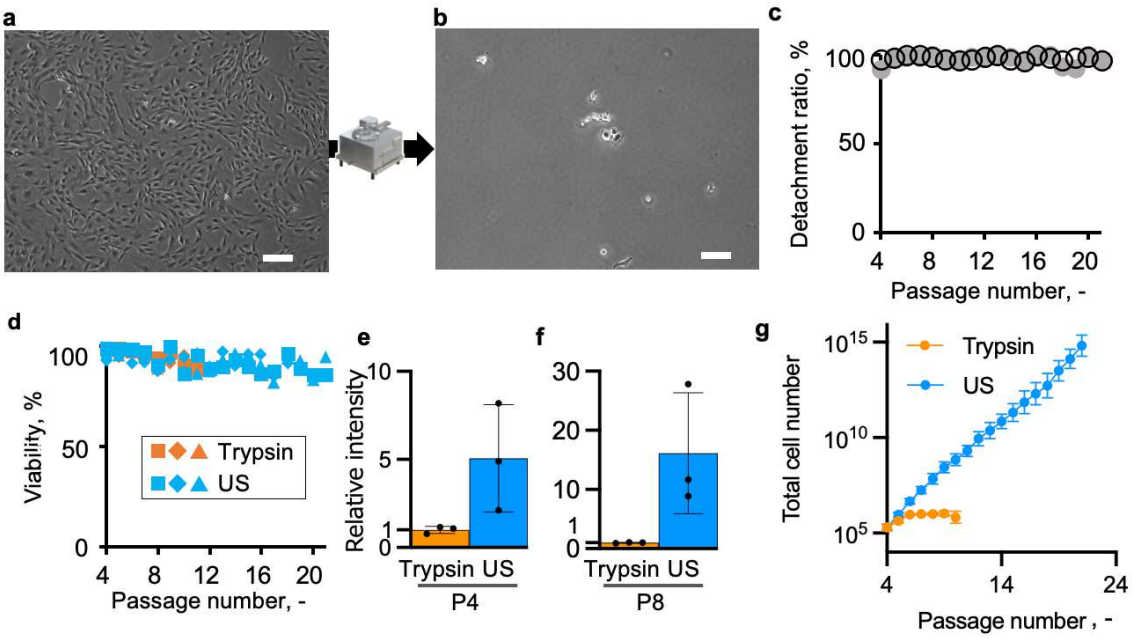


Fig. 3 | Ultrasound-mediated enzyme-free passaging enables efficient cell harvesting and sustained long-term expansion of MSCs.

(a) Phase-contrast image of mesenchymal stromal cells (MSCs) before detachment. Scale bar: 200 µm.

(b) Culture surface after ultrasound-mediated enzyme-free passaging. Cells were effectively detached, leaving only negligible residual cells on the substrate. Scale bar: 200 µm.

(c) Time course of cell detachment efficiency under ultrasound stimulation (N = 2). Effective detachment was consistently achieved at all passages examined.

(d) Viability of MSCs after ultrasound-mediated enzyme-free passaging (US) or conventional trypsinization (Trypsin). High cell viability was maintained in both groups.

(e, f) Western blot analysis of fibronectin (FN) levels immediately after detachment at passages P4 and P8 (N = 3). Although no statistically significant difference was detected between the groups, a trend toward higher FN retention was observed in the US group.

(g) Cumulative numbers of MSCs serially passaged using ultrasound-mediated enzyme-free passaging (US) or trypsinization (Trypsin), plotted on a logarithmic scale. Data are presented as the mean ± SD from independent experiments, with passage-dependent sample sizes (Trypsin: N = 3 up to P10; US: N = 3 up to P18 and N = 2 at passages P19–P21).

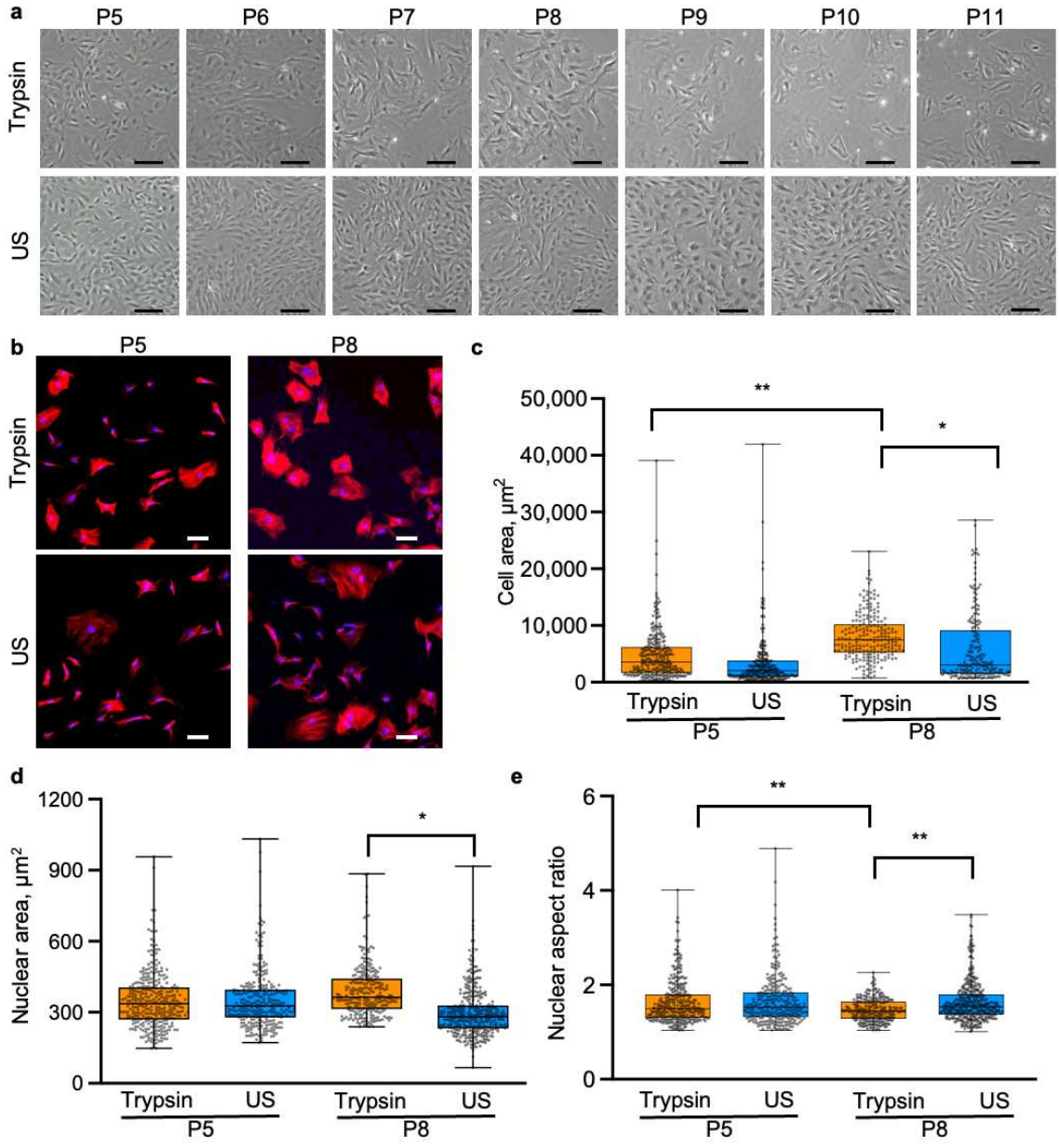


Fig. 4 | Ultrasound-mediated enzyme-free passaging preserves cellular and nuclear morphology during long-term MSC expansion.

(a) Phase-contrast images of MSCs serially passaged using conventional trypsinization (Trypsin) or ultrasound-mediated enzyme-free passaging (US) at the indicated passages. Scale bar: 200 µm. (b) Representative fluorescence images of filamentous actin (red) and nuclei (blue) in MSCs cultured under Trypsin or US passaging conditions. Scale bar: 100 µm. (c–e) Quantitative analysis of cell area, nuclear area, and nuclear aspect ratio, respectively (N = 3). Two-way ANOVA was performed to assess the main effects of passaging method and passage number, as well as their interaction. When a significant main effect or interaction was detected, post hoc were conducted using Tukey's test. Asterisks indicate statistically significant differences (*$P < 0.05$, **$P < 0.01$).

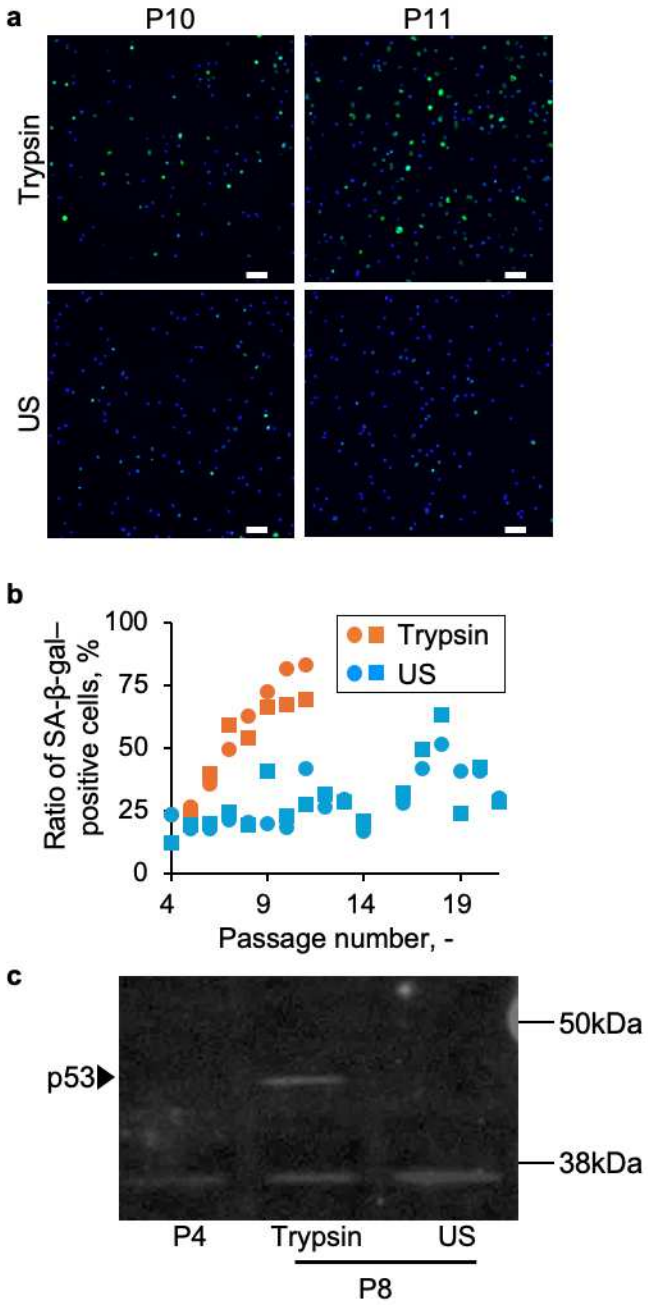


Fig. 5 | Evaluation of cellular senescence markers in MSCs during long-term serial passaging. (a) Representative images of SA-β-Gal staining in MSCs serially passaged using trypsinization (Trypsin) or ultrasound-mediated enzyme-free passaging (US). SA-β-Gal–positive cells are shown in green, and nuclei (Hoechst) are shown in blue. Scale bar: 100 μm. (b) Quantification of the percentage of SA-β-Gal–positive cells (N = 2). (c) Representative western blot analysis of p53 expression after long-term passaging. Additional independent experiments and quantitative analyses are provided in the Supplementary Information.

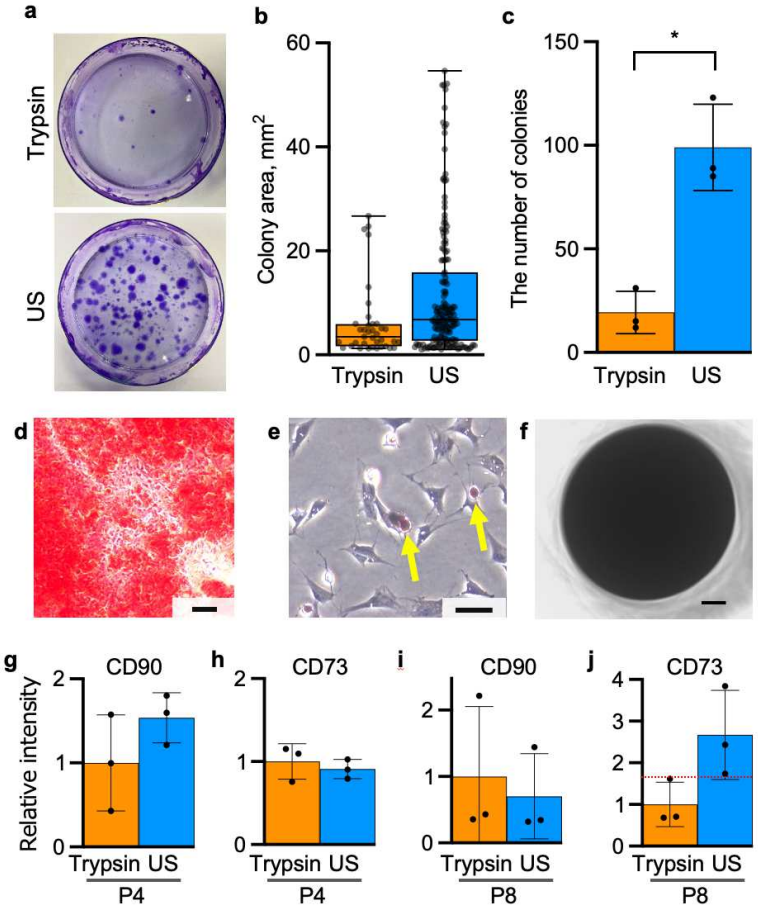


Fig. 6 | Maintenance of stemness in MSCs after serial ultrasound-mediated enzyme-free passaging.

(a) Representative images and quantification of colony formation assays (N = 3). Additional images are provided in the Supplementary Information. (b) Distribution of colony area at passage 8 (P8). Each dot represents a single colony; boxes indicate the interquartile range, center lines indicate the median, and whiskers indicate the minimum and maximum values (N = 3). (c) Quantification of the number of colonies per dish. Bars represent the mean, error bars indicate the standard deviation, and dots represent independent experiments (N = 3). Asterisks indicate statistically significant differences (*P < 0.05). (d) Osteogenic differentiation assessed by Alizarin Red S staining at passage 8 (P8). Scale bar: 200 µm. (e) Adipogenic differentiation assessed by Oil Red O staining at passage 8 (P8). Yellow arrows indicate intracellular lipid droplets. Scale bar: 50 µm. (f) Chondrogenic differentiation assessed by Alcian Blue staining at passage 8 (P8). Scale bar: 200 µm. (g, h) Western blot analysis of CD90 and CD73 expression at passage 4 (P4) (N = 3). (i, j) Western blot analysis of CD90 and CD73 expression at passage 8 (P8) (N = 3).

Supplementary Files

This is a list of supplementary files associated with this preprint. Click to download.

- supplementdataARRIVEXXXchecklistfinal.docx
- UltrasoundmediatedecmpreservingdetachmentXXXSIXXXv2.pdf